Received: 12 July 2021 | Revised: 29 August 2021 | Accepted: 31 August 2021
DOI: 10.22034/ecc.2021.299439.1216
Eurasian Chemical Communications
SAMI

FULL PAPER

Synthesis, characterization and evaluation of inhibition corrosion of bacterial cellulose/metal oxides nanocomposites

Sraa Hussein Kreydie* |**Basim I. Al-Abdaly***

Department of Chemistry, College of Science, University of Baghdad, Baghdad, Iraq

***Corresponding Authors:**
Sraa Hussein Kreydie
Basim I. Al-Abdaly
Email:basim.ibrahim@sc.uobaghdad.edu.iq
sraa.kreydie1205@sc.uobaghdad.edu.iq
Tel.: +009647704664573

The present study aimed at synthesizing and characterizing mixed oxides/bacterial cellulose nanocomposites and evaluating its Anti-corrosion. The first part of this experimental work included preparation of bacterial cellulose, and syntheses and characterization of [NBC/ZnO:CuO] and [NBC/NiO:CuO] nanocomposites based on nanostructure specifically with bacterial cellulose as a composite. All the composites were synthesized using hydrothermal method; the structures of the new composites were characterized by Fourier transform infrared, scanning electron microscopy–energy dispersive X–ray (SEM/EDX), x-ray diffraction (XRD) and Atomic force microscopy (AFM). The second part of study pertains to the evaluation of Anticorrosion. It was noticed that the highest inhibition efficiency was for NBC/ ZnO:CuO and NBC/NiO:CuO where in inhibition efficiency was 97.31% and 93.37%, respectively, due to lower corrosion current density which reduced corrosion rate.

KEYWORDS

Bacterial cellulose; nanocomposites; hydrothermal method; anticorrosion.

Introduction

Nanocomposites have attracted great interest in both industry applications and academic studies. They often exhibit remarkable improvement in materials properties when compared with virgin polymer or conventional micro and macro-composites [1]. Polymer nanocomposites are innovative two-phase composite materials in which polymers and fillers strengthen each other. Polymer nanoparticles composites are created by incorporating a small weight percentage of nanoparticles (ten percent) into a polymer matrix [2,3]. The filled polymers' scattered particles are in the nanometer range. Fillers improve the mechanical, optical, and thermal properties of the polymer when compared with the virgin polymer [2,4].

Bacterial cellulose (BC) is an intriguing, long-lasting and Nano fibrous biodegradable material with almost the same chemical structure (a polysaccharide consisting of a 14-unit D-glucose linear chain) and crystalline structure like cellulose derived from plants [5,6]. BC fibers, on the other hand, have a diameter of a few (40–70) nm and exhibit a number of distinct features, containing high purity, polymerization degree, crystallinity, which leads to high strength, and modulus. 1–5 BC membranes have a high water-holding capacity due to their small fiber diameter, which results in a large surface area and extremely porous structure [7].

Copper, zinc and nickel oxides nanoparticles are widely utilized in the synthesis of nanocomposites with cellulosic materials and polymers; zinc oxide has high binding energy, fast photo catalysis, and great thermal properties [8,9], whilst copper has good electrical, optical, and chemical characteristics, whilst NiO NPs is an important metal oxide with cubic lattice structure, used in a variety of applications such as catalysis, battery cathodes, gas sensors, electrochromic films and magnetic materials. It can also be extensively used in dye sensitized photocathodes [10]. These metals and metal oxides are environmentally beneficial, as well as inexpensive in cost, non-toxic, and readily available commercially.

This work reported the synthesis of nanocomposites from bacterial cellulose and some oxides in a new formula, to enhance the ability of bacterial cellulose to be used as an alternative for many industrial applications, by preparing it by hydrothermal method and testing its anti-corrosion efficacy.

Materials and methods

All materials, chemicals and the instrumentation used in the current work include: The use of prepared bacterial cellulose of type *Gluconacetobacter xylinus* ATCC 53582 (American culture type group, Manassas, VA, USA) [11], fabricate and characterization of mixed oxides with bacterial cellulose (BC) as nanocomposites [BC/NiO:CuO] and [BC/ZnO:CuO] within 12 hours; the composites mentioned above were synthesized using hydrothermal method.

Synthesis of bacterial cellulose/ nickel oxide and copper oxide nanocomposite [NBC/NiO:CuO]

3.1 g from Ni(CH3COO)2.4H2O was dissolved in 25 mL of Deionized (DI) water to make a solution of 0.5 M. This solution was added to 4.6 g from bacterial cellulose with stirring for 1 h, 2.27 g from Cu(CH3COO)2.2H2O dissolved in 25 mL of deionized water to make a solution of 0.5 M. Then, the second solution to was added the first solution with continuous stirring for 20 minutes; after that 2 mL of NaOH 0.5 M was added to the last solution, followed by heating the mixture by (~150 °C) for 12 hours with heating rate = 2 °C /min).

The cell was cooled and separated by centrifugation the 4000 (rpm). After that, the separated sample was washed three times with deionized water and dried at 59 °C.

Synthesis of bacterial cellulose /zinc oxide and copper oxide [NBC/ ZnO: CuO] nanocomposite within 12 hour

0.5 g from Zn(CH3COO)2.2H2O was dissolved in 25 mL of Deionized (DI) water to make a solution of 0.2 M. This solution was added to 4.6 g from bacterial cellulose with stirring for 1h, 2.27 g from Cu(CH3COO)2.2H2O dissolved in 25 mL of deionized water to make a solution of 0.5 M. Then, the second solution was added to the first solution with continuous stirring for 20 minutes. After that 2 mL of NaOH 0.5 M was added to the last solution, followed by heating the mixture by (~150 °C) for 12 hours with heating rate = 2 °C/min). The cell was cooled and separated by centrifugation the 4000 (rpm). After that, the separated sample was washed three times with deionized water and dried at 59 °C.

Results and discussion

Atomic force microscopy (AFM)

AFM images in two dimensions (2D) and three dimensions (3D) were obtained for viewing bacterial cellulose nanocomposites/metal oxides, where the metal oxides consist of metals (Cu, Zn, Ni) as oxides which reveals the topography, particles distribution and average diameter for all composites synthesized via chemical protocol (hydrothermal method). The grooves are not homogenous as depicted by three dimensional image, which is mainly due to agglomeration nanoparticles of the

cellulose surface, showing that the diameter of the particle was in average of 50.00 nm for [bacterial cellulose/ZnO:CuO] nanocomposite (Figure 1A). And for [bacterial cellulose/NiO:CuO] nanostructure (Figure 2B), the average diameter was shown to be 73.99 nm.

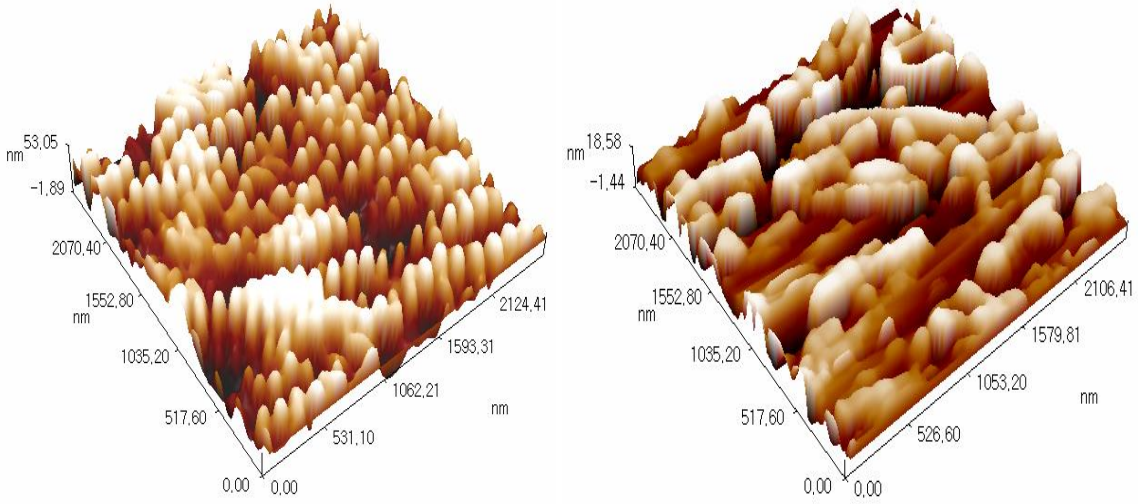

FIGURE 1 (2D and 3D) AFM images of A: [NBC/ NiO:CuO], B:[NBC/ ZnO:CuO] nanostructure composite by hydrothermal method

Surface morphology analysis via SEM, EDX techniques synthesized of composites [NBC/ metal oxides] nanostructured

The morphology of the synthesized [NBC/ZnO:CuO] was investigated by SEM, EDX along with mapping its components, as shown in Figure 2A. The SEM for [NBC/ZnO:CuO] indicates the formation of sheets nanostructured, along with mapping of ZnO:CuO, carbon and oxygen that shows distribution of particles of each element on the sample surface. EDX spectrum shows the rise of peak intensity of copper by 81.9%, oxygen by 5.2%, and carbon by 12.9%; however, there is no value for zinc oxide, which is due to the presence of a large proportion of copper oxides covering the surface of bacterial cellulose in this nanocomposite [12]. The SEM analysis of [NBC/NiO:CuO] nanocomposite is shown in Figure 2B, along with mapping of NiO:CuO that shows the distribution of particles of each nanoparticles on the sample surface. Its EDX spectrum displayed shows the rise in peak intensity of copper peak by 51.2%, carbon by 8.2%, oxygen by 18.6% and nickel peak by 22.0%. Ni:Cu concentration does not show significant gradients from one area to another [13]. This result indicates the formation of [BC/NiO:CuO] composite nanostructures.

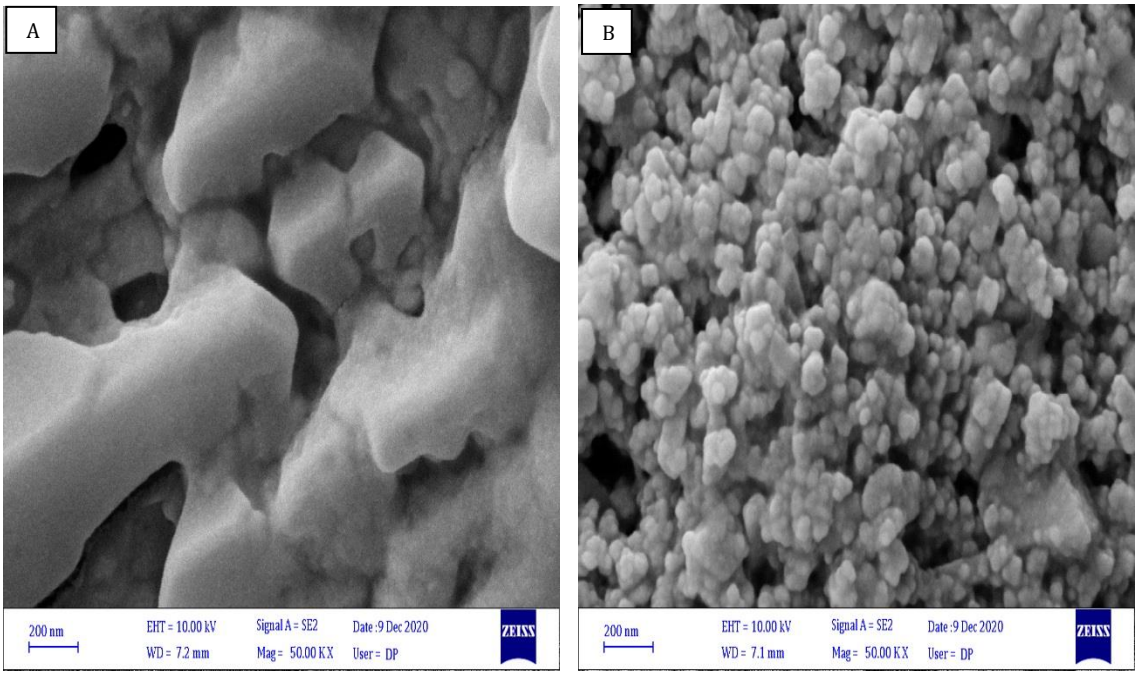

FIGURE 2 Surface morphology of nanocomposites (A) SEM image of fine crystal of [NBC/NiO:CuO] (B) SEM image of fine crystal of [NBC/ZnO:CuO]

Analysis of FT-IR spectral data for bacterial cellulose/metal oxides nanocomposites synthesized

The FTIR spectrum of [NCB/ZnO: CuO] nanoparticle composite is reported in Figure 3, illustrating the FTIR spectrum of bacterial cellulose and copper:zinc oxides nanocomposites synthesizing the characteristic vibrational bands at 3461-3346 cm^{-1} stretching of (O-H), 2401-2337 cm^{-1} stretching of (C-H). It refers to the expansion of non-symmetric of alkanes of CH2, 1622 cm^{-1} deformity of OH, 1384 cm^{-1} deformation of CH2, 1163 cm^{-1} stretch of C-O-C, 1087 cm^{-1} stretch of CC and CO, 1232 cm^{-1} deformity of CH. The band at 2360 cm^{-1} in the bacterial cellulose/zinc:copper compound indicated wavenumbers are lower when the synthesis time is longer, which suggests strong interaction between the copper and hydroxyls sites of bacterial cellulose. It is worth mentioning that BC/Cu-Zn compound synthetized appears at typical peaks of Cu oxides. Typically, this spectrum appears at the peaks matching to 675, 644 and 576 cm^{-1}, all these peaks indicate the vibrations of copper oxide vibrational peaks[14]. In addition, zinc oxides are present at the ranges of 422-453cm^{-1} [15].

While the FTIR spectrum of [NBC/NiO:CuO] nanoparticle composite is reported in Figure 4, it should be noted that the broad band at 3444-3367 cm^{-1} indicates the bands (Oxygen–hydrogen) stretching vibrations and the bands weak at 1629-1622 cm^{-1} that are assigned to H–O–H. The reason for the formation of these weak bands is attributed to the absorption of water when preparing the FTIR sample in the open air. This indicates the effect of the presence of water molecules in the sample structure. The broad band at 690-655 cm^{-1} is attributed to NiO stretching vibration; these bands indicate the presence of nickel oxide on the surface of bacterial cellulose, so that NiO nanoparticles have their IR peak of Ni–O stretching vibration and shift to blue direction [16]. The FTIR spectrum of CuO peaks at 520-501 cm^{-1} reveals the formation of CuO [17].

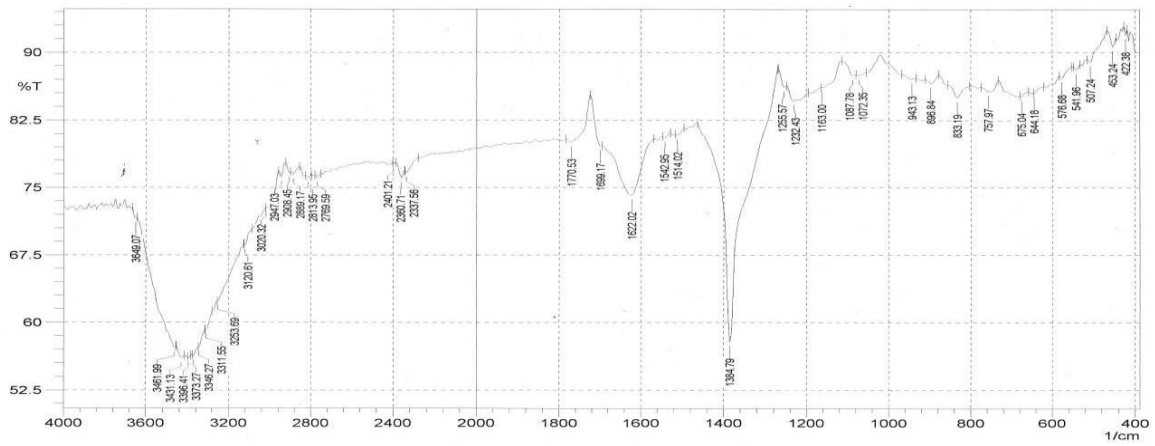

FIGURE 3 FT-IR spectrum of [NBC/ZnO:CuO] nano composite

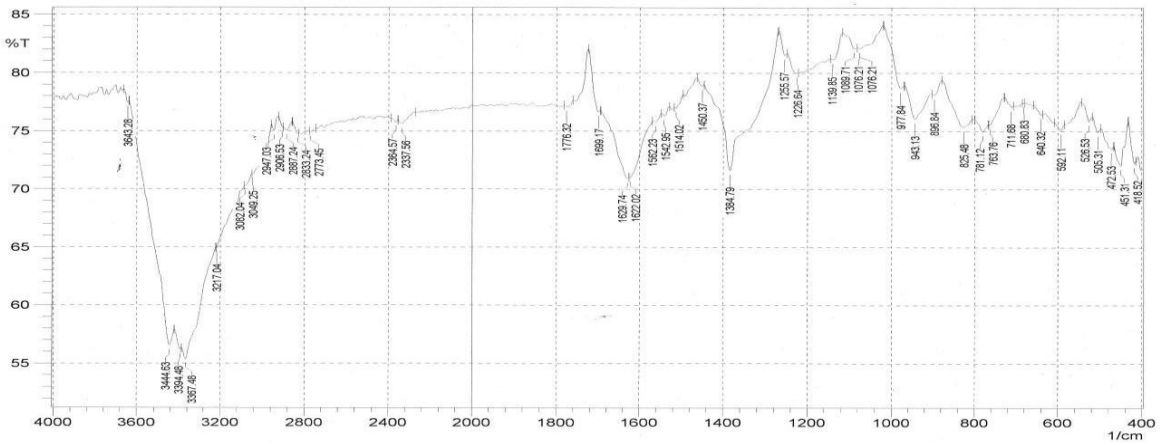

FIGURE 4 FT-IR spectrum of [NBC/NiO:CuO] nano composite

X-Ray diffraction of bacterial cellulose/metal oxides nanocomposites

Figure 5 shows the XRD pattern of [NBC/ZnO:CuO] nanostructure that is describing the featured peaks of bacterial cellulose covered with copper oxides and zinc oxides nanoparticles. The diffraction peaks appeared at 32.6º, 35º and 37.7º corresponding to (313) and (021) and (404) planes values, respectively [18]. The average particle size of the [NBC/ZnO:CuO] nanocomposite was 26.52 nm.

The XRD pattern of [NBC/NiO:CuO] nanostructure (Figure 6), exhibited diffraction peaks at (39°, 46°), representing the planes (610, 122) respectively [15]; these planes represent the face centered cubic (FCC) according to standard JCPDS card number (00-001-1142). The mean particle size of [NBC/NiO:CuO] nanoparticles was calculated and found to be 70.13 nm.

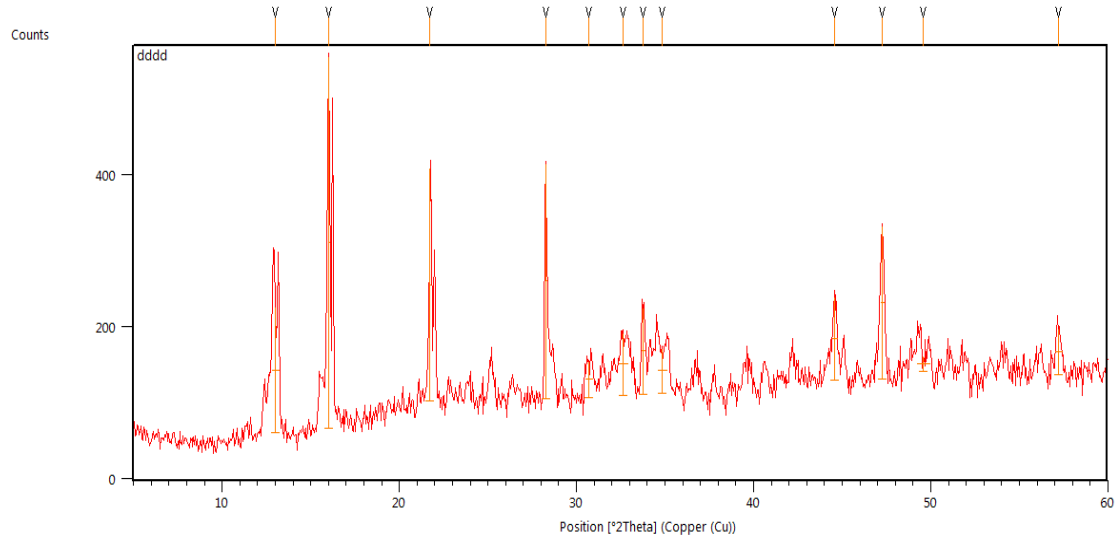

FIGURE 5 XRD pattern of [NBC/ZnO:CuO] nanostructure

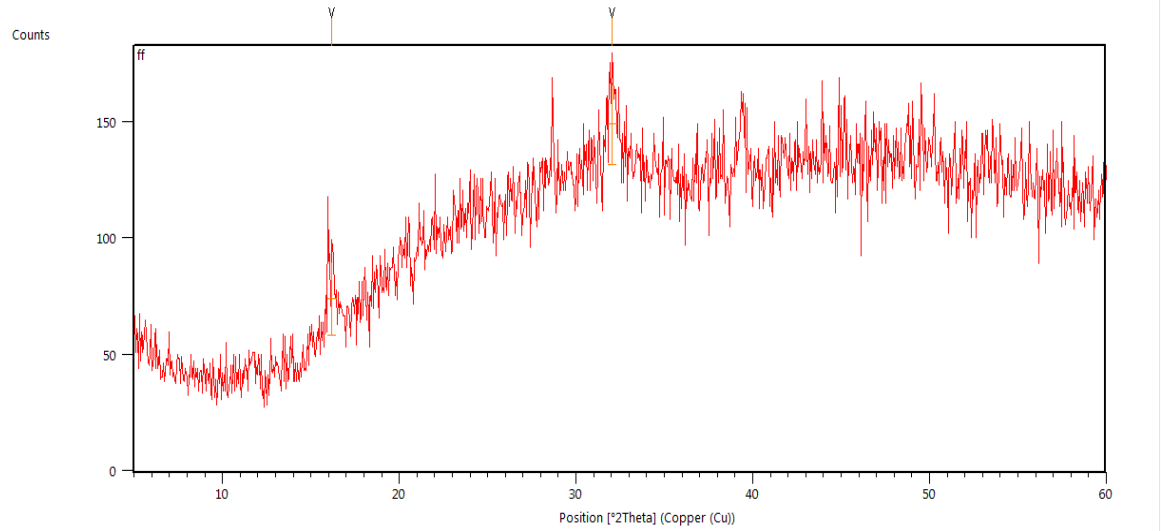

FIGURE 6 XRD pattern of [NBC/NiO:CuO] nanostructure

Inhibition of carbon steel corrosion by synthesized nanocomposites (using the hydrothermal method)

It can be observed from the obtained results (Table 4.1) that the synthesized nanocomposites showed good inhibition efficiency against carbon steel corrosion.

This inhibition is due to the physical adsorption of NBC/ZnO:CuO and NiO:CuO nanoparticles on the carbon steel surface [19].

Metal ions coordinated with the compound are expected to operate the electron pairs based on the binding atoms, while the atoms of the compound substance are ready in this case to bind with the carbon surface atoms, thus protecting the surface from corrosion. Also, it was noticed that the highest inhibition efficiency was for NBC/ZnO:CuO and NBC/NiO:CuO, where in the inhibition efficiency was 97.31% and 93.37%, respectively, due to lower corrosion current density which reduces corrosion rate, and the lowest inhibition efficiency (6.95%) belonged to NBC/NiO:ZnO using the auxiliary microwave method, due to the generation of high corrosion current density, which resulted in a higher corrosion rate.

TABLE 1 Electrochemical data of the carbon steel alloy corrosion in sea water (3.5%NaCl) for the synthesized composites (hydrothermal method)

Sample	Hours (hydrothermal)	Ecorr. (mV)	Icorr. (μA/cm²)	-βc (mV/sec)	βa (mV/sec)	W.L (g/m².d)	P.L (mm/y)	IE%
Blank		-830.7	312.19	-290.7	45.7	7.80	3.62	-
NBC/NiO:CuO	12	-885.7	20.67	-57.6	28.8	5.12	2.38	93.37
NBC/ZnO:CuO	12	-355.6	8.32	-25.9	25.8	2.08	9.66	93.37

This inhibition is due to the physical adsorption of NBC/ZnO:CuO and NiO:CuO nanoparticles on the carbon steel surface can be seen in Figure 7 polarization curve of carbon steel alloy in sea water (3.5%NaCl) using the synthesized composites as inhibitors.

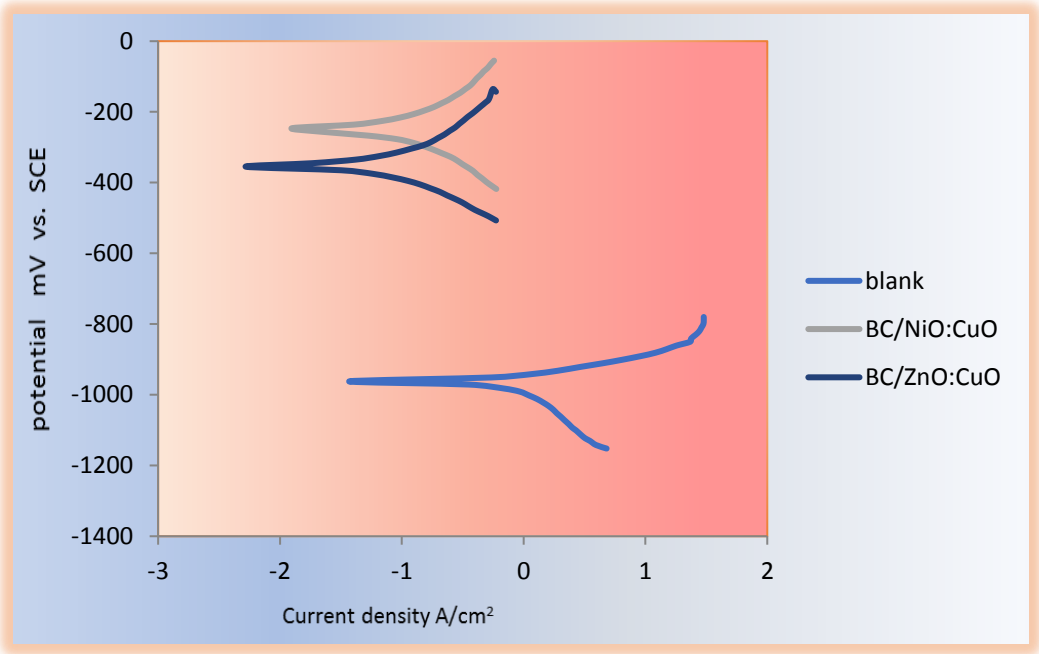

FIGURE 7 Polarization curve of carbon steel alloy in sea water (3.5%NaCl) using the synthesized composites as inhibitors

Generally, the oxidation demeanor of the metal will form an inert layer (metal oxide) on the surfaces of the biodegradable polymeric film, which prevents ions from spreading throughout the electrolyte solution [20].

This is due to the porous nature of the bacterial cellulose film, which cannot prevent hostile ions in the solution from spreading, allowing the electrolyte to easily concentrate in the bacterial cellulose film. The obtained results in Figure 8 showed better corrosion resistance in bacterial cellulose/metal oxide and thorny membranes. This effect is attributed to the metal's high affinity for oxygen, which allows for rapid oxidation, and the metal oxide provides a strong barrier to polymeric film surfaces. The total results revealed that increasing concentrations of metallic nano-oxide in the coating resulted in improved effectiveness of corrosion.

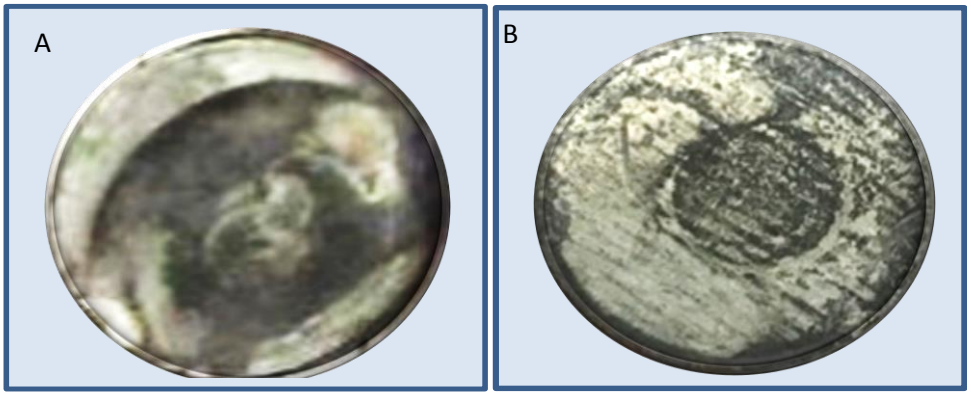

A: NBC/ NiO:CuO composite B: NBC/ ZnO:CuO composite

FIGURE 8 Carbon steel alloys ingots after corrosion.(hydrothermal method)

Conclusion

In conclusions, better behavior of corrosion resistance was in bacterial cellulose/metal oxide and thorny membranes. This effect is attributed to the metal's high affinity for oxygen, which allows for rapid oxidation, and the metal oxide provides a strong barrier to polymeric film surfaces. The total results revealed that increasing concentrations of metallic nano-oxide in the coating resulted in improved effectiveness of corrosion.

Acknowledgements

I would like to thank all member staff of department of Chemistry, University of Baghdad.

References

[1] A. Sangwan, P. Malik, R. Gupta, R.K. Ameta, T.K. Mukherjeed, Nanocomposites: Preparation, Characterization, and Applications, *Nanotechnology*, Jenny Stanford Publishing, **2021**, 201-247. [Pdf], [Google Scholar], [Publisher]

[2] B. Rajeswari, N. Malarvizhi, D. Prakash, S.N. Jaisankar, *J. Thermoplast. Compos. Mater.*, **2020**, *33*, 1555-1568. [crossref], [Google Scholar], [Publisher]

[3] R.A. Faris, Z.F. Mahdi, M.D.A. Husein, *Immobilised Gold Nanostructures on Printing Paper for Lable-Free Surface-enhanced Raman Spectroscopy*, IOP Conference Series: Materials Science and Engineering, IOP Publishing, **2020**, *871*, p 012019. [crossref], [Google Scholar], [Publisher]

[4] P.H.C. Camargo, K.G. Satyanarayana, F. Wypych, *Mat. Res.*, **2009**, *12*, 1-39. [crossref], [Google Scholar], [Publisher]

[5] K. Qiu, A.N. Netravali, *Polym. Rev.*, **2014,** *54,* 598-626. [crossref], [Google Scholar], [Publisher]

[6] H. Ullah, H.A. Santos, T. Khan, *Cellulose*, **2016,** *23,* 2291-2314. [crossref], [Google Scholar], [Publisher]

[7] H. Ullah, F. Wahid, H.A. Santos, T. Khan, *Carbohydr. Polym.,* **2016,** *150*, 330-352. [crossref], [Google Scholar], [Publisher]

[8] S.H. Ferreira, M. Morais, D. Nunes, M.J. Oliveira, A. Rovisco, A. Pimentel, H. Águas, E. Fortunato, R. Martins, *Materials*, **2021**, *14*, 2385. [crossref], [Google Scholar], [Publisher]

[9] R.A. Faris, S.K. Al-Hayali, A.H. Al-Janabi, *Opt. Commun.*, **2021**, *485*, 126746. [crossref], [Google Scholar], [Publisher]

[10] M. El-Kemary, N. Nagy, I. El-Mehasseb, *Mater. Sci. Semicond. Process.*, **2013**, *16*, 1747-1752. [crossref], [Google Scholar], [Publisher]

[11] Z. Shi, S. Zang, F. Jiang, L. Huang, D. Ma, Y. Lu, G. Yang, *RSC Adv.*, **2012,** *2*, 1040-1046. [crossref], [Google Scholar], [Publisher]

[12] M. Wasim, M.R. Khan, M. Mushtaq, A. Naeem, M. Han, Q.J.C. Wei, *Coatings.*, **2020,** *10*, 364. [crossref], [Google Scholar], [Publisher]

[13] N. Phutanon, K. Motina, Y.H. Chang, S. Ummartyotin, *Int. J. Biol. Macromol.*, **2019**,

136, 1142-1152. [crossref], [Google Scholar], [Publisher]
[14] C.W. Tang, C.B. Wang, S.H. Chien, **2008**, *Thermochim. Acta*, *473*, 68-73. [crossref], [Google Scholar], [Publisher]
[15] I.M. Araújo, R.R. Silva, G. Pacheco, W.R. Lustri, A. Tercjak, J. Gutierrez, J.R.S. Júnior, F.H.C. Azevedo, G.S. Figuêredo, M.L. Vega, S.J.L. Ribeiro, H.S. Barud, *Carbohydr. Polym*., **2018**, *179*, 341-349. [crossref], [Google Scholar], [Publisher]
[16] H. Qiao, Z. Wei, H. Yang, L. Zhu, X. Yan, **2009**, *2009*, Article ID 795928, 1-5. [crossref], [Google Scholar], [Publisher]
[17] M. Elango, M. Deepa, R. Subramanian, A.M. Musthafa, **2018**, *57*, 1440-1451. [crossref], [Google Scholar], [Publisher]
[18] Z. Wang, Y.H. Lee, B. Wu, A. Horst, Y. Kang, Y.J. Tang, D.R. Chen, *Chemosphere*, **2010,** *80*, 525-529. [crossref], [Google Scholar], [Publisher]
[19] R. Solmaz, E. Altunbaş, G. Kardaş, *Mater. Chem. Phys.*, **2011**, *125*, 796-801. [crossref], [Google Scholar], [Publisher]
[20] S. Lyon, *Nucl Sci Eng*, **2012**, 3-30. [crossref], [Google Scholar], [Publisher]

How to cite this article: Sraa Hussein Kreydie*, Basim I. Al-Abdaly*, Synthesis, characterization and evaluation of inhibition corrosion of bacterial cellulose/metal oxides nanocomposites**.** *Eurasian Chemical Communications*, 2021, 3(10), 706-714. **Link:** http://www.echemcom.com/article_136614.html